

Optimization of carbon dioxide absorption in a continuous bubble column reactor using response surface methodology

Ayşe Gul¹  | Masoud Derakhshandeh² | Umran Tezcan Un³

¹Department of Civil Engineering, Abdullah Güл University, Kayseri, Turkey

²Civil Engineering Department, İstanbul Gelişim University, İstanbul, Turkey

³Department of Environmental Engineering, Eskisehir Technical University, Eskisehir, Turkey

Correspondence

Ayşe Gul, Civil Engineering Department, Abdullah Güл University, Kayseri 38080, Turkey.

Email: ayse.gul@agu.edu.tr

Funding information

Anadolu University, Grant/Award Number: 1706F386

Abstract

Carbon dioxide absorption using amine based solvents is a well-known approach for carbon dioxide removal. Especially with the increasing concerns about greenhouse gas emissions, there is a need for an optimization approach capable of multifactor calibration and prediction of interactions. Since conventional methods based on empirical relations are not efficiently applicable, this study investigates use of Response Surface Methodology as a strong optimization tool. A bubble column reactor was used and the effect of solvent concentration (10.0, 20.0 and 30.0 vol%), flow rate (4.0, 5.0 and 6.0 L min⁻¹), diffuser pore size (0.5, 1.0 and 1.5 mm) and temperature (20.0, 25.0 and 30.0°C) on the absorption capacity and also overall mass transfer coefficient was evaluated. The optimization results for maintaining maximum capacity and overall mass transfer coefficient revealed that different optimization targets led to different tuned operational factors. Overall mass transfer coefficient decreased to 34.7 min⁻¹ when the maximum capacity was the desired target. High reaction rate along with the highest absorption capacity was set as desirable two factor target in this application. As a result, a third scenario was designed to maximize both mass transfer coefficient and absorption capacity simultaneously. The optimized condition was achieved when a gas flow rate of 5.9 L min⁻¹, MEA solution of 29.6 vol%, diffuser pore size of 0.5 mm and temperature of 20.6°C was adjusted. At this condition, mass transfer coefficient reached a maximum of 38.4 min⁻¹, with a forecasted achievable absorption capacity of 120.5 g CO₂ per kg MEA.

KEYWORDS

bubble column reactor, carbon dioxide absorption, mass transfer coefficient, process optimization, response surface methodology

1 | INTRODUCTION

Amines are well-known solutions for scrubbing acid gases since their first introduction by Bottoms in 1930 (Roger, 1930). Carbon dioxide is considered as the most significant greenhouse gas, responsible for global warming with an estimated 80% contribution (Lashof & Ahuja, 1990; Pszczółkowski et al., 2015). Current efforts to accomplish

the sustainable use of carbon dioxide (CO₂) as a chemical feedstock address three major concerns of our time: Strategies for combating climate change, the transition from conventional to renewable sources of energy, and the sustainable use of raw materials. One of the essential elements in reaching the world's sustainable development goals is the suggestion that anthropogenic greenhouse gas (GHG) emissions be reduced (Pszczółkowski et al., 2015).

Absorption, adsorption and photoconversion of CO₂ (Fadillah & Saleh, 2022; Saleh, 2022a, 2022b), membrane, chemical looping, and geothermal and biochemical technologies are currently one of the most effective techniques for reducing CO₂ emissions. Different approaches available for carbon dioxide capture include post-combustion, pre-combustion and oxy-fuel approaches (D'Alessandro et al., 2010). Conventional methods of using amines for absorbing carbon dioxide emissions of a power plant while being well studied and highly efficient, increase the consumed energy of the plant by 25%–40% mainly during regeneration step (D'Alessandro et al., 2010).

Aqueous solution of amines and mixtures of amine based chemicals with other additives have been studied by researchers including N-methyl-2-pyrrolidone (NMP), monoethanolamine (MEA) (Aronu et al., 2011; Putta et al., 2017; Yeh et al., 2001; Yuan & Rochelle, 2018) triethanolamine (TEA) (La Rubia et al., 2010), methyldiethanolamine (MDEA) and piperazin (PZ) (Ali & Aroua, 2004; Navaza et al., 2009; Pashaei et al., 2017), 2-amino-2-methyl-1-propanol (AMP) (Choi et al., 2009), diethylethanolamine (DEEA) and Ethylethanolamine (EEA) (Chen & Liao, 2014; Vaidya & Kenig, 2009), alkaline solutions (Chen et al., 2008; Li et al., 2014; Sada et al., 1985; Tippayawong & Thanompongchart, 2010), ammonia solution (Shuangchen et al., 2016).

Chemical absorption as a post-combustion carbon dioxide removal method has been commonly studied because of their high removal efficiency, simplicity in application with retrofitting existing facilities, energy efficiency and low environmental impacts (Benson & Orr, 2008; D'Alessandro et al., 2010; Peng et al., 2012).

Although the method is being actively used to remove carbon dioxide from natural gas in sweetening process but their use for carbon dioxide capture as a byproduct of combustion is still waiting for future developments of the method (D'Alessandro et al., 2010). It was reported that for conventional absorbents like MEA to absorb CO₂ from flue gas in power plants would increase the cost of investment by 60% for lower net energy output of the plant and capital investment cost where the reduction of cost with promising solvent combinations like CESAR-1 was not considerable as well (Manzolini et al., 2015). Any modification in the efficiency of any step of the method will reduce the estimated costs where different technologies have been studied for CO₂ capture (Fadillah & Saleh, 2022; Saleh, 2022a, 2022b).

Many studies have shown the significant effect of multiple factors for both the nature of absorbents and the process variables. MEA based absorbents are still the most efficient absorbents with reported absorption capacities of 60 to 120 g CO₂/kg solution being equal to 0.5 mol CO₂/mole amine to 0.7 mol CO₂/mole amine (Bernhardsen & Knuutila, 2017). The major tested reactor types were bubble column (Adeosun et al., 2013; Chen et al., 2015; La Rubia et al., 2010; Navaza et al., 2009; Sada et al., 1985), packed bed (Aroonwilas & Veawab, 2004; Choi et al., 2009; Tippayawong & Thanompongchart, 2010; Yeh et al., 2001). The suggested range for operating temperature varies between literatures. For MEA solution, Yeh et al. concluded insignificant effect of temperature between 38.0 and 54.0°C on the removal efficiency

(Yeh et al., 2001). This was also confirmed elsewhere for the range of 25–45°C (Chen et al., 2015).

Although generally the effect of variables like gas flow rate, temperature and absorbent capacity is known, the interaction effect of the variables cannot be revealed unless a robust statistical approach implemented. A very well-tuned model helps to find optimized condition. The novel approach in this study is the implementation of RSM methodology for optimization of the process in a continuous approach. For optimization approaches many different methods are being implemented by researchers for removal of variable chemical components (Azari et al., 2021; Azari et al., 2022; Dashtian et al., 2017; Nazerdey-lami & Zare-Dorabe, 2019) while RSM is one of the most implemented methods (Saleh et al., 2017; Sebeia et al., 2019). The scale of the process is also a pilot set-up with efficient mass flow meter for gas and liquid which is very sensitive result for such studies.

Although generally the effect of variables like gas flow rate, temperature and absorbent capacity is known, the interaction effect of the variables cannot be revealed unless a robust statistical approach implemented. A very well-tuned model helps to find optimized condition

In the present study, the effect of four substantial factors including gas flow rate, absorbent concentration, diffuser pore size and temperature was studied following an optimization studies using Response Surface Methodology with Box-Behnken model. The methodology is considered as a powerful tool for multivariable processes responses and their optimization (Dean et al., 2017; Jaafari et al., 2018).

2 | THEORY AND CALCULATIONS

2.1 | Absorption capacity calculations

The area over the CO₂-time profile graph (Exhibit 3) corresponds to the total absorbed CO₂. The input flow rate of CO₂ was known from total flow rate and the inlet concentration. The outlet flow rate of CO₂ was calculated based on the fixed flow rate of N₂ which was an inert compound and the read CO₂ concentration. The following relation was

used to calculate the CO₂ outlet flow;

$$Q_{CO_2out} = Q_{total,in} \cdot Y_{N2in} \left(\frac{Y_{CO_2out}}{Y_{N2out}} \right) \quad (1)$$

The volumetric flow rates were converted to molar mass flow rate using conversion factors and assuming ideal gas equation of state where each mole at standard temperature and pressure (STP) of 1 atm and 273.0 K occupies 22.4 L. This was corrected for adjusted temperature. Then the concentration (ppm)-time graph was replotted for mass flow rate-time.

The volumetric flow rates were converted to molar mass flow rate using conversion factors and assuming ideal gas equation of state where each mole at standard temperature and pressure (STP) of 1 atm and 273.0 K occupies 22.4 L

The rate of absorbed CO₂ at each reading interval was then calculated using following equation;

$$R_{CO_2} = \dot{M}_{CO_2,in} - \dot{M}_{CO_2,out} \quad (2)$$

The amount of absorbed CO₂ for each time interval was calculated using following equation;

$$M_{CO_2ab} = R_{CO_2} \times (t_2 - t_1) \quad (3)$$

The absorption capacity of the absorbent was calculated using below equation;

$$Ab.Cap = \frac{\sum_1^n M_{CO_2ab}}{M_{MEA}} \quad (4)$$

Where n is the number of time intervals, M_{CO₂} is the mass of absorbed CO₂ and M_{MEA} is the mass of MEA in the solution.

Spreadsheets in MS Excel was used for calculation procedures.

2.2 | Overall mass transfer (K_Ga) calculation

Estimation of overall mass transfer coefficient in gas/liquid systems depends on the rate of reaction in the liquid phase and the trans-

fer in the gas phase. In MEA/CO₂ systems, the overwhelming transfer direction is from the gas phase to the liquid (Exhibit 1) where the reaction in the liquid phase is fast which means the process is not being controlled by the reaction rate between CO₂/MEA. The fast reaction of CO₂/MEA is explained elsewhere in the literature on the mechanism of the chemical reaction (Lv et al., 2015). It is assumed that two-film model is used to determine the mass transfer coefficient and to define the mass transfer of CO₂. According to two film model, equilibrium is assumed at the interface. According to two film model, the local absorption rate, expressed as total mass transfer coefficients, on both the gas and liquid side at a local point, can be written as follows;

$$r_A = (K_G a) \cdot (C_g - HC_L) \quad (5)$$

We assume a plug flow for the gas phase and well mixed flow for liquid phase, steady state, mass equilibrium with z;

Mass balance over ΔZ :

$$(U_g C_g)_z^S - (U_g C_g)_{z+\Delta z}^S = r_A \Delta V \quad (6)$$

$$\Delta V = \Delta Z \cdot S \quad (7)$$

Where S is the column cross-sectional area.

Combining Equations (5) with (6);

$$(U_g C_g)_z \cdot S - (U_g C_g)_{z+\Delta z} \cdot S = K_G a \cdot (C_g - HC_L) (\Delta Z \cdot S) \quad (8)$$

$$\frac{S \cdot U(C_{gz} - C_{gz+\Delta z})}{\Delta z} = K_G a \cdot (C_g - HC_L) \cdot S \quad (9)$$

The term C_g ≫ HC_L is acceptable because both Henry coefficient and C_L are low at the range of this application (Chen et al., 2015).

$$S \cdot U \frac{dC}{dz} = S \cdot K_G a \cdot (C_g) \quad (10)$$

$$Q \frac{dC}{C} = S \cdot K_G a \cdot dz \quad (11)$$

$$Q \int_{Cin}^{Cout} \frac{dC}{C} = \int_0^{L+\Delta L} S \cdot K_G a \cdot dz \quad (12)$$

$$K_G a = \frac{Q_g \cdot \ln \frac{C_0}{C}}{(\Delta L + L) \cdot S} \quad (13)$$

Where C_g is CO₂ gas concentration in gas phase (mol L⁻¹), C_L, CO₂ gas concentration in liquid phase (mol L⁻¹), r_A is absorption rate (mol L⁻¹ min⁻¹), K_Ga is overall mass-transfer coefficient (min⁻¹), S is the column

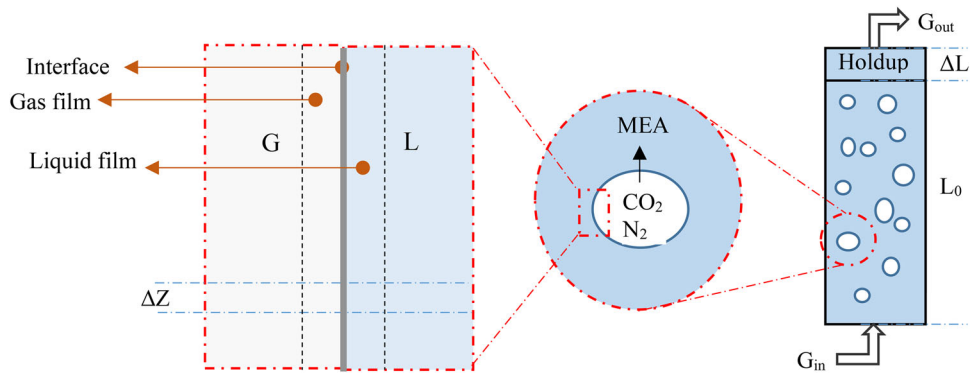


EXHIBIT 1 The schematic of two film theory for CO_2 absorption in MEA.

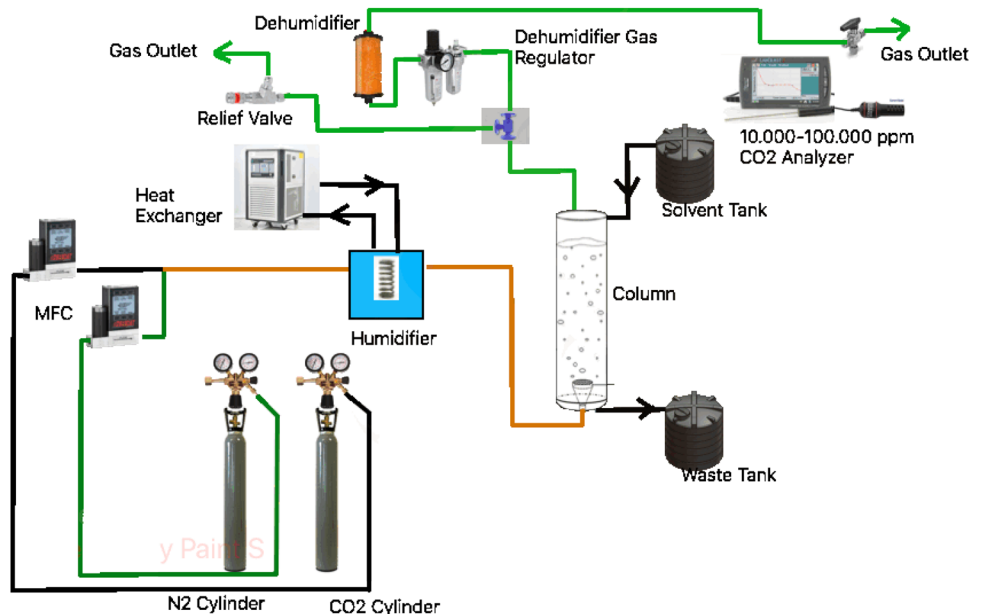


EXHIBIT 2 The experimental setup.

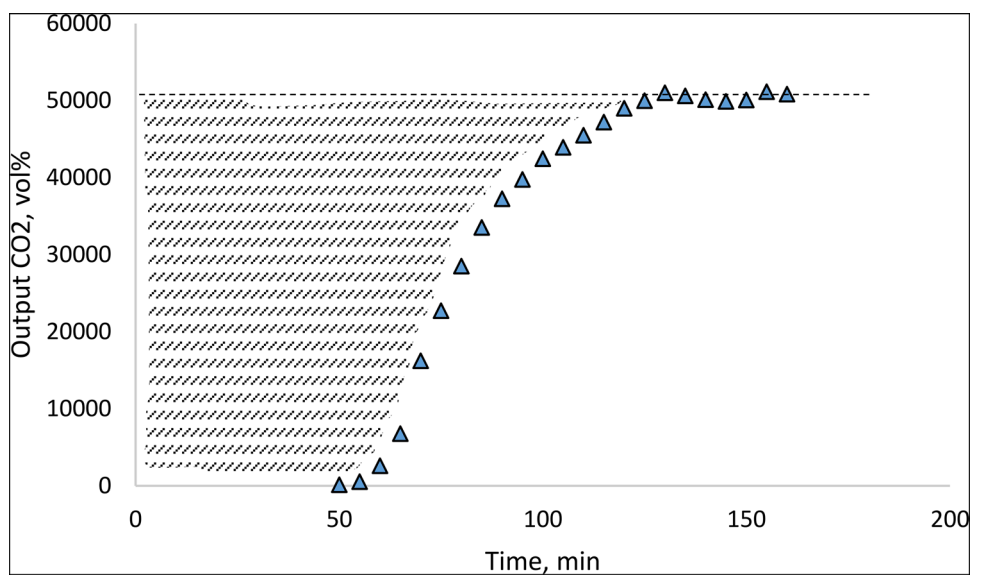


EXHIBIT 3 A sample of the CO_2 concentration profile at the output.

EXHIBIT 4 Build Information of experiment design with input factors.

Study type	Response surface		Subtype	Randomized			
Design type	Box-Behnken		Runs	27			
Design model	Quadratic		Blocks	No Blocks			
Factor	Name	Units	Type	Min	Max	Mean	Std. Dev.
A	Gas flow	L.min ⁻¹	Numeric	4.0	6.0	5.0	0.6794
B	Absorbent conc.	(%)	Numeric	10.0	30.0	20.0	6.79
C	Diffuser Pore size	mm	Numeric	0.5	1.5	1.0	0.3397
D	Temperature	C	Numeric	20.0	30.0	25.0	3.40

EXHIBIT 5 The adjusted variables for different runs and experimental responses.

Run	A: Gas flow	B: Abs. conc.	C: Diff. Pore size	D: Temp.	R1: Abs Cap.	R2: KGa
	L min ⁻¹	(%)	mm	°C	g CO ₂ /kg Sol	min ⁻¹
1	5.0	30.00	0.5	25.00	102.1	32.9
2	5.0	20.00	1.0	25.00	66.6	24.5
3	6.0	10.00	1.0	25.00	32.7	22.2
4	5.0	10.00	1.0	20.00	37.8	17.0
5	6.0	30.00	1.0	25.00	101.3	37.3
6	5.0	10.00	0.5	25.00	36.2	30.3
7	4.0	30.00	1.0	25.00	96.0	26.3
8	5.0	20.00	1.0	25.00	66.7	24.2
9	5.0	10.00	1.5	25.00	41.5	16.3
10	5.0	30.00	1.0	30.00	96.4	32.1
11	4.0	20.00	1.5	25.00	72.6	19.9
12	4.0	20.00	1.0	30.00	74.6	23.2
13	5.0	20.00	1.5	20.00	62.1	18.9
14	5.0	20.00	1.5	30.00	88.4	24.0
15	4.0	20.00	1.0	20.00	62.5	17.0
16	5.0	20.00	0.5	20.00	74.1	30.4
17	4.0	10.00	1.0	25.00	27.0	26.2
18	4.0	20.00	0.5	25.00	59.8	25.5
19	6.0	20.00	0.5	25.00	41.4	34.8
20	6.0	20.00	1.5	25.00	75.6	27.6
21	5.0	30.00	1.0	20.00	119.3	24.3
22	5.0	30.00	1.5	25.00	110.5	23.3
23	5.0	10.00	1.0	30.00	40.2	23.6
24	5.0	20.00	1.0	25.00	70.3	32.0
25	5.0	20.00	0.5	30.00	68.0	30.4
26	6.0	20.00	1.0	30.00	73.7	37.1
27	6.0	20.00	1.0	20.00	71.1	28.1
28	5.0	20.00	0.5	25.00	74.7	30.4

cross section area (cm²), U is gas superficial velocity (m s⁻¹) and Q is the gas flow rate (L min⁻¹). In Equation (13), ΔL is the liquid hold-up as shown in the Exhibit 1, C_0 and C are the gas concentration in the inlet and outlet respectively.

2.3 | Chemical reaction mechanism

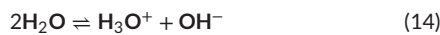
The reaction mechanism in a ternary system of H₂O-CO₂-amine differs based on the number of amine functionality. The following reactions

EXHIBIT 6 ANOVA for response surface reduced quadratic model for R1.

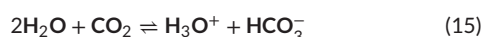
Source	Sum of Squares	df	Mean Square	F-value	p-value	Estim. Coef
Model	5983.11	14	427.36	20.68	< 0.0001	
Intercept		1				11.55
A-Gas flow	0.2985	1	0.2985	0.0144	0.9063	0.2728
B-Absorbent conc.	5445.92	1	5445.92	263.54	< 0.0001	3.42
C-Diffuser Pore size	156.10	1	156.10	7.55	0.0177	0.3285
D-Temperature	7.50	1	7.50	0.3628	0.5582	0.1482
AB	0.1112	1	0.1112	0.0054	0.9427	-0.0886
AC	46.14	1	46.14	2.23	0.1609	-0.1749
AD	8.85	1	8.85	0.4283	0.5251	-0.2362
BC	0.6141	1	0.6141	0.0297	0.8660	0.0065
BD	58.13	1	58.13	2.81	0.1193	-0.5403
CD	99.83	1	99.83	4.83	0.0483	0.7694
A ²	49.07	1	49.07	2.37	0.1493	-0.2679
B ²	2.13	1	2.13	0.1032	0.7535	-0.3127
C ²	0.9209	1	0.9209	0.0446	0.8364	0.3059
D ²	55.67	1	55.67	2.69	0.1267	0.3925
Residual	247.97	12	20.66			
Lack of Fit	244.52	10	24.45	14.18	0.0676	

which are equilibrium reactions have been suggested for single amine functionality as for MEA (Aronu et al., 2011):

Water dissociation:



Carbon dioxide dissociation:



Bicarbonate dissociation:



Dissociation of protonated MEA:



Carbamate reversion to bicarbonate:



3 | MATERIALS AND METHOD

3.1 | Chemicals

Deionized water was supplied using a Thermo Scientific, Germany unit with ultra pure filters. MEA was supplied by Sigma (Germany).

N₂ (>99.99%, 200 bar) and CO₂ (>99.95%, 150 bar) gas cylinders was purchased from Oksan gas, Turkey.

3.2 | Methodology

The absorption column is depicted in **Exhibit 2**. The column has a height of 1.0 m and diameter of 5.0 cm. The process was run in semi batch mode where liquid did not flow and the gas phase was flowing through the solution. For each run, the temperature of the water circulation bath was adjusted on the desired temperature and run for almost 20.0 min to ensure stable temperature on the vessel wall. A 1 L MEA solution is used in each experiment. The MEA solution was prepared in parallel and put over hot plate to maintain the desired temperature and quickly charged into column and left for 10 min to stabilize the temperature. The gas mixture was supplied using two separate mass flow controllers (ALICAT Scientific Mass Flow Controller, Range: 0.0–10.0 L min⁻¹, accuracy: 0.2% of full-scale) for nitrogen and carbon dioxide. The gas mixture was first directly sent to CO₂ analyzer to ensure initial 50,000 ppm concentration then the main line valves was opened and gas mixture directed to the column filled with MEA solution. The gas mixture was bubbled first in a humidifier where its temperature was controlled/adjusted by a heat exchanger in a closed loop. The humidified gas mixture was bubbled using diffuser in the column and the carbon dioxide concentration in the gas phase in the output was monitored using a Vernier CO₂ gas sensor (USA). The process continued until there was no further absorption. This was confirmed

EXHIBIT 7 ANOVA for response surface reduced quadratic model for R2.

Source	Sum of squares	df	Mean square	F-value	p-value	Estim. Coef
Model	120.51	14	8.61	85.00	0.0007	
Intercept						0.6972
A-Gas flow	3.04	1	3.04	29.99	0.0003	-0.0137
B-Absorbent conc.	13.59	1	13.59	134.16	0.0005	-0.0128
C-Diffuser Pore size	78.12	1	78.12	771.35	0.0001	0.0136
D-Temperature	4.92	1	4.92	48.53	0.0028	-0.0093
AB	0.0471	1	0.0471	0.4652	0.5951	-0.0030
AC	0.1122	1	0.1122	1.11	0.9303	-0.0004
AD	0.0420	1	0.0420	0.4150	0.8214	0.0010
BC	3.39	1	3.39	33.52	0.2182	-0.0056
BD	0.0256	1	0.0256	0.2528	0.7740	0.0013
CD	0.9506	1	0.9506	9.39	0.2936	-0.0047
A ²	0.5813	1	0.5813	5.74	0.9476	-0.0003
B ²	0.0009	1	0.0009	0.0088	0.2223	0.0049
C ²	11.87	1	11.87	117.20	0.8992	0.0005
D ²	0.0151	1	0.0151	0.1495	0.3456	0.0036
Residual	1.11	11	0.1013			
Lack of Fit	0.0006	10	0.0001	0.4316	0.8510	not significant

by the concentration/time profile as shown in **Exhibit 3** for a specific run.

3.3 | Experimental design

A Response Surface Methodology using Box-Behnken model was implemented as was also previously implemented elsewhere in optimization attempts for experimental and also industrial case studies (Hemmati & Rashidi, 2019; Rahimi et al., 2017; Sahraie et al., 2019). The detail of the specifications and range of input variables are presented in **Exhibit 4**. The input variables of interest were gas flow rate (4.0, 5.0 and 6.0 L min⁻¹), absorbent concentration (10.0, 20.0 and 30.0 vol%), diffuser pore size (0.5, 1.0 and 1.5 mm) and temperature (20.0, 25.0 and 30.0°C). The responses as are summarized in **Exhibit 5** where the absorption capacity and the overall volumetric mass transfer coefficient K_{Ga} are calculated using Equations (4) and (17), respectively.

Design Expert software was used for data analysis. The response behavior was predicted using a second degree quadratic model for both responses. The applied general model was as follows;

$$\begin{aligned} R^{\lambda} = & c_1 A + c_2 B + c_3 C + c_4 D + c_5 AB + c_6 AC + c_7 AD + c_8 BC \\ & + c_9 BD + c_{10} CD + c_{11} A^2 + c_{12} B^2 + c_{13} C^2 + c_{14} D^2 + R_0 \end{aligned} \quad (19)$$

Where R is the responses being absorption capacity and K_{Ga} and A, B, C and D are input variables (**Exhibit 4**), c1–c4 are linear factors coeffi-

cients, c5–c10 are the coefficients for two-factor interactions, c11–c14 are second degree factors coefficients and R₀ is the intercept.

4 | RESULTS AND DISCUSSION

4.1 | Statistical evaluations

A total number of 27 runs were conducted. The maximum absorption capacity was 119.3 g CO₂/kg MEA when gas flow 5.0 L min⁻¹, absorbent concentration 30.0 vol%, diffuser pore size 1.0 mm and temperature of 20.0°C were adjusted. The worst case where the lowest absorption capacity of 27.0 g CO₂/kg MEA was recorded when conditions of gas flow 4.0 L min⁻¹, absorbent concentration 10.0 vol%, diffuser pore size 1.0 mm and temperature of 25.0°C were adjusted. The highest estimated overall mass transfer coefficient K_{Ga} was 10.6 min⁻¹ at gas flow rate 5.0 L min⁻¹, MEA 30.0%, 1.5 mm pore size and temperature of 25.0°C. Box-Behnken model gives multiple repeats at central points where for the same equilibrium conditions (i.e. Temperature, MEA% in solution, CO₂% in gas phase and pressure), it was observed that different capacities were obtained. As for example runs nos. 2, 8, 11, 18, 19, 20, 24 and 28 have the same equilibrium variables but the obtained capacity results fall in a wide range of 41.4 to 74.7 g CO₂/kg MEA. It shows that process variables are also very significant factors. It can be related to the different hold-up and formation of extra pressure at higher flow rates which means equilibrium factors are not maintained constant. Our results also show that pore sizes were significant variable on the absorption capacity of the solution.

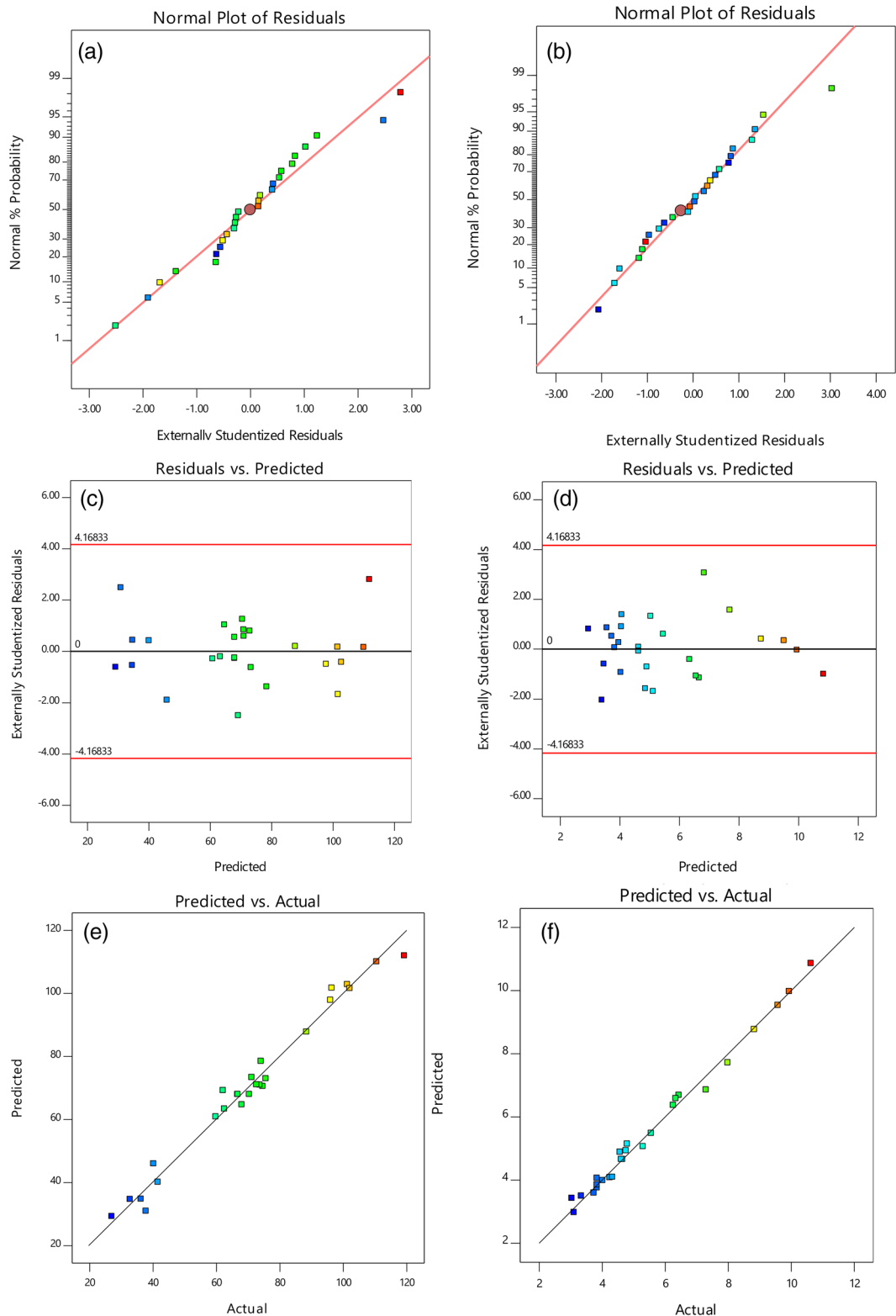


EXHIBIT 8 The diagnostic plots of (a) Normal plot of residuals for R1, (b) Normal plot of residuals for R2, (c) Externally studentized residuals versus predicted values for R1, (d) Externally studentized residuals versus predicted values for R2, (e) Predicted versus actual responses for R1, (f) Predicted versus actual responses for R2.

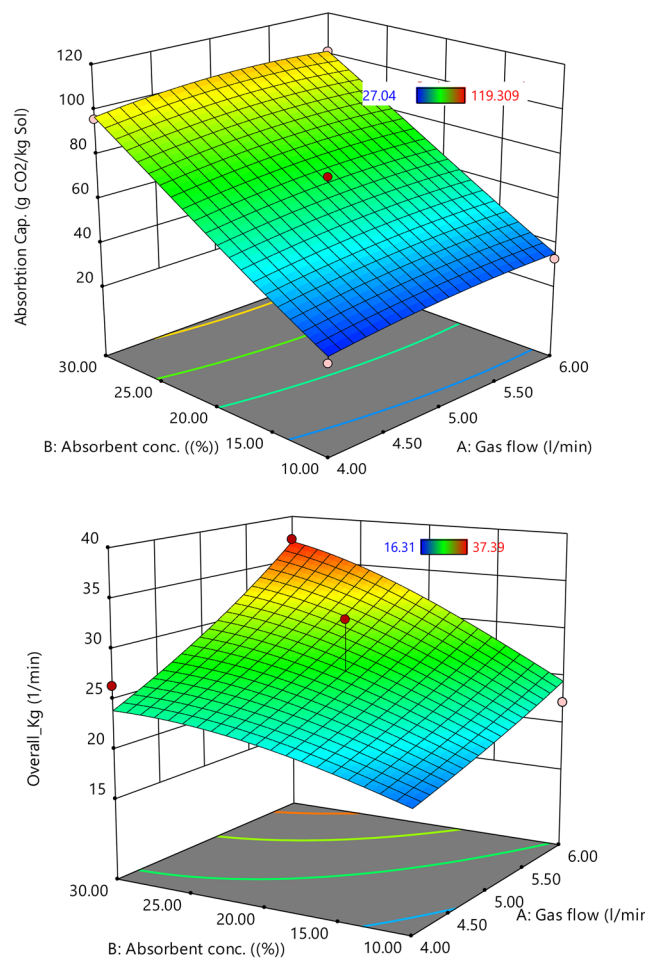


EXHIBIT 9 3D plot of absorption capacity, K_{GA} and holdup versus gas flow rate and absorbent concentration at temperature: 25.0°C; diffuser pore size: 1.0 mm.

Reported data on the equilibrium of CO₂-Water/MEA in the literature (Aronu et al., 2011; Liu et al., 1999), includes a saturation step and then measurement of the vapor pressure at a fully batch mode. It is not trustworthy to be used as a reference for evaluating continuous processes were all geometries are significant factors.

The model terms and the Fraction of Design Space (FDS) statistics as provided in *Supplementary file* ensures the robustness of the model and its reasonable prediction power for both responses. The variance inflation factor for defined parameters were very close to the ideal value of 1.0. The R^2 squares were also close to zero for all factors. For a response surface design, a FDS graph is a better metric for evaluation. This graph shows that more than 98% of the design space falls below standard error of 1.0 which is very confidential when knowing that the average of the response was in the range of 27–120. The model also showed no aliases.

4.2 | Analysis of variance (ANOVA)

The results for ANOVA test are summarized in Exhibits 6 and 7. It was confirmed that the models were significant with $p\text{-value} < 0.0001$. The

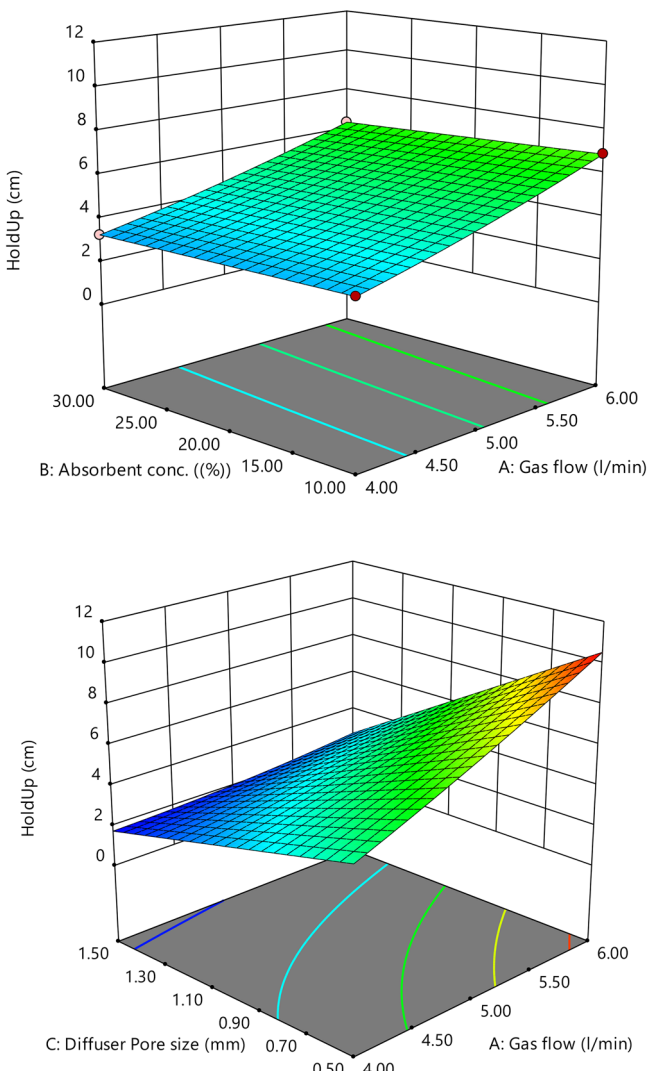


EXHIBIT 10 Holdup at different conditions of gas flow rate, diffuser and MEA concentration.

defined parameters had p -values less than 1.0 which showed moderate significance. There was no significant lack of fit for both response models. In a quadratic model, a variable is represented in different terms, for example for variable A, different term including A, AB, A² and AC are included in the model. Therefore, in this kind of studies, overall performance of a model is aimed to be significant rather than single terms.

Diagnostic plots are depicted in Exhibit 8. The normal plot of residuals in Exhibit 8 showed approximately reasonable linearity with just one outlier in run 19 for R1 and two outliers for R2 in run 17 and 24. These points were excluded from evaluation and the plots are the final pose of models (Exhibit 8). The plot of externally studentized residuals versus predicted values in Exhibit 8 showed a random bounce around zero line with almost a horizontal band without any outliers. The plot of predicted value versus actual value in Exhibit 8 shows the models ability to predict responses since the points are scattered in a linear pattern. Therefore, it was concluded that the proposed model was a very good description of experimental data. The best λ for a power transformation for R1 was 0.66 (Equation (23)). The estimated

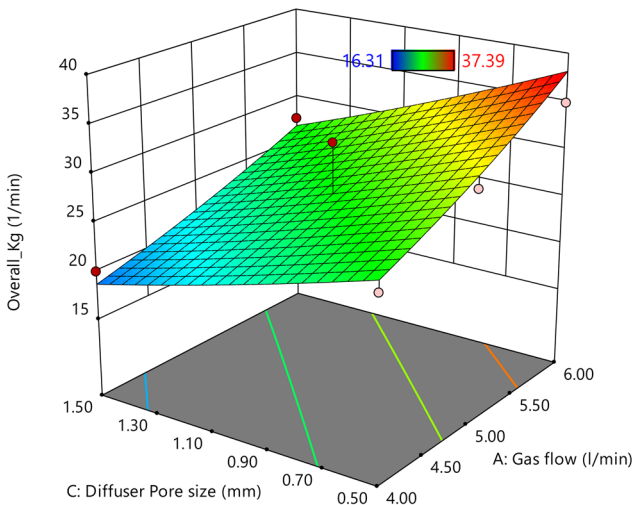
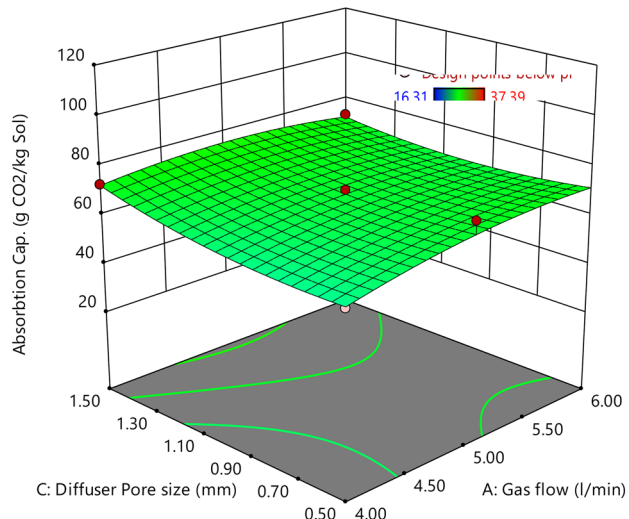


EXHIBIT 11 3D plot of absorption capacity versus gas flow rate and diffuser pore size at temperature: 25.0°C; absorbent concentration: 20.0 vol%.

coefficients for the quadratic models to be applied in Equation (23) are listed in Exhibits 6 and 7.

4.3 | The effect of gas flow rate

The three dimensional (3D) plot of models for absorption capacity and overall mass transfer coefficient against gas flow rate is given in **Exhibit 9**. The graph was plotted at diffuser pore size of 1.0 mm and temperature of 25.0°C. The gas flow rate change at the range of 4.0–6.0 L min⁻¹ did not show substantial change in absorption capacity but was effective on overall mass transfer coefficient (**Exhibit 9**). The slightly dome like appearance of the plot reveals that there is an optimum value for gas flow rate in the range of 4.0–6.0 L min⁻¹ which gives the highest absorption capacity. The influence of gas flow rate factor was not high because for example when pore size was fixed at 1.0 mm

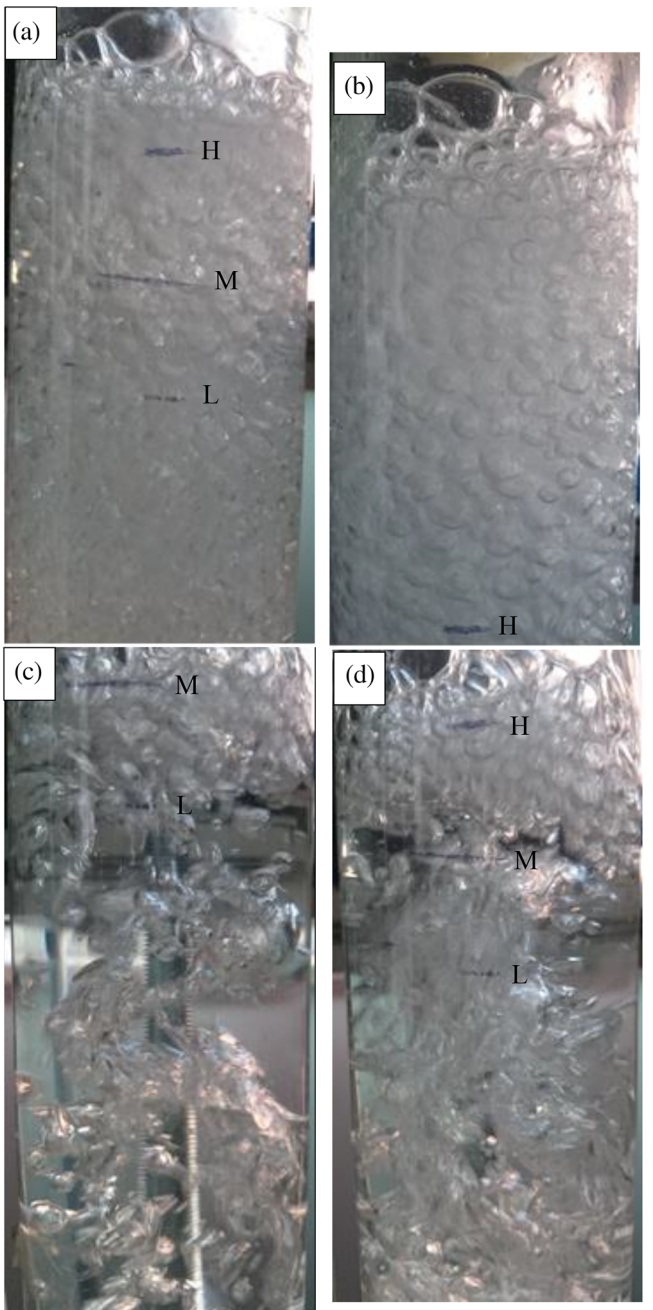


EXHIBIT 12 Photograph of bubbles in the column, (a) Q: 4.0 L min⁻¹, Pore: 0.5 mm, MEA 10.0%, (b) Q: 6.0 L min⁻¹, Pore: 0.5 mm, MEA 10.0%, (c) Q: 4.0 L min⁻¹, Pore: 1.5 mm, MEA 10.0%, (d) Q: 6.0 L min⁻¹, Pore: 1.5 mm, MEA 10.0%.

the difference between max and min was only 10% (62.6 vs. 68.8 g CO₂/kg MEA). It is because the absorption capacity of the solvent is more related to the chemistry of the solution and available absorbent rather than physical factors.

The gas flow rate had positive effect on the K_{Ga} where higher flow rates has improved K_{Ga}. There was almost a 53% increase in K_{Ga} when flow rate was increased from 4.0 to 6.0 L min⁻¹ at higher absorbent concentrations. By considering the holdup graph in **Exhibit 10** shows that hold up has increased with flow rate but not significantly affected

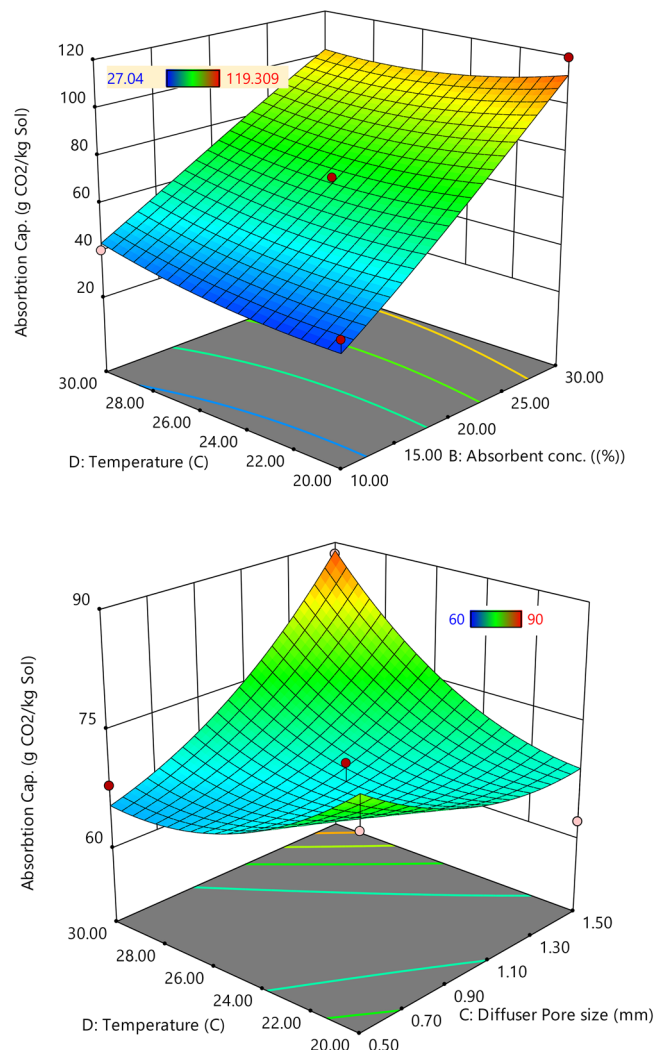


EXHIBIT 13 3D plot of absorption capacity versus temperature, diffuser pore size and MEA concentration.

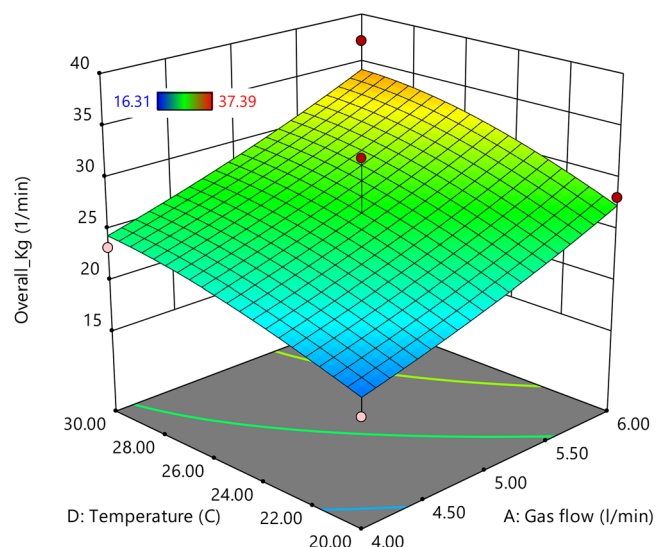


EXHIBIT 14 The effect of Temperature on K_{GA} at different gas flow rates with pore size: 1 mm, MEA 20.0 vol%.

by concentration. This is to say, higher flow rates provides a longer contact pass which along with higher turbulences resulted in improved mass transfer rates. From Equation (17) it is clear that the K_{GA} is in direct relation with gas flow rate but in reverse relation with hold up. The increase of flow rate almost linearly increases the holdup (Exhibit 10) but since the total liquid head do not increase to the same proportion, K_{GA} shows significant increase with gas flow rate. High flow rates provides higher turbulences which is a favorable effect.

4.4 | The effect of absorbent concentration

The 3D plots in Exhibit 9 shows the effect of absorbent concentration. As can be seen, absorption capacity is strongly dependent on the solvent concentration where higher concentrations greatly increased the capacity. As for the variation of 10.0 to 30.0 vol% of absorbent concentration, the capacity increased from around 35–101 g CO_2 per kg of MEA. The positive effect of increased absorbent concentration is actually expected because it directly means more available reactant MEA and more capacity potentially to be filled with carbon dioxide. This is actually a kinetically important factor rather than being a process variable unlike other factors including gas flow rate, diffuser diameter and temperature.

Exhibit 9 also reveals that absorbent concentration had major effect on K_{GA} where for a gas flow rate of 4.0 L min^{-1} , the K_{GA} has improved by 60% when absorbent concentration was increased from 10.0 to 30.0 vol%. It can be concluded that higher MEA concentration not only means higher capacity but also results higher mass transfer rate. This is in consistent with the work of Maceiras et al. (2008). MEA concentration showed little effect on holdup (Exhibit 10). The insignificant effect of MEA concentration on holdup was also confirmed for all pore sizes as shown in Exhibit 10. Higher MEA concentration in the liquid phase keeps the concentration gradient of CO_2 in the liquid film high for a longer time so that the rate of mass transfer will stay higher over reaction period. The mass transfer will stop when there is no unreacted MEA molecule in the liquid phase.

4.5 | The effect of diffuser pore size

The results of absorption capacity at different diffuser pore sizes are presented in Exhibit 11. The graph was plotted at absorbent concentration of 20.0 vol% and temperature of 25.0°C . Regarding pore size, in general, small pores close to 0.5 mm showed better performance regarding transfer rate but this factor was not so determining for absorption capacity.

The overall mass transfer coefficient was strongly affected by pore size (Exhibit 11). The plot of hold up versus pore size in Exhibit 10 shows that there is an opposite relation between holdup and pore size where wider pores resulted in lower holdup. The smaller pore size has significantly improved the overall mass transfer coefficient. For a gas flow rate of 5.0 L min^{-1} , the decrease of pore size from 1.5 to

EXHIBIT 15 Solutions for best input data in optimized condition.

Target	Q_g $L\ min^{-1}$	MEA vol%	Pore size mm	Temp. °C	Abs. Cap. (g CO ₂ /kg)	K _{Ga} (1/min)	Holdup	Desirability
K _{Ga} Max	6.0	25.8	0.8	27.3	85.4	38.4	8.1	1
Cap. Max	5.7	29.9	0.6	20.3	121.3	34.7	8.3	1
K _{Ga} and Cap. Max	5.9	29.6	0.5	20.6	120.5	37.5	9.9	1

EXHIBIT 16 Comparison of this study with most relevant previous optimization studies.

Opt.Methd	Absor.	CO ₂ (%)	Pore size (mm)	Temp. (°C)	Abs.Cap. (g CO ₂ /kg solv.)	K _{Ga} (kmol/h m ³ kPa)	Process	Ref.
BBD	MEA	5	0.5	20.6	120.5	0.91	bc**	This study
CCD	Piperazine	12-40	1.0	n.a*	101.2	n.a	bc. with mixer	(Pashaei et al., 2020)
BBD	MEA-MeOH	5-15	n.a	45.0	n.s	4.98	pc***	(Rashidi et al., 2020)
BBD	MEA + Glycerol	10	n.a	35.4	n.s	0.63	pc	(Valeh-e-Sheyda & Barati, 2021)

*Not applicable

**Bubble column

***Packed column.

0.5 corresponded to 42.9% increase in K_{Ga}. This can be mathematically discussed using Equation (13) where for a constant gas flow rate at wider diffuser pore resulted in lower gas hold up (Exhibit 12) and since according to Equation (17) there is a reverse relation between K_{Ga} and holdup, the bigger pore size results in higher K_{Ga}. The physical explanation of the phenomenon could be as the big pore size results in extremely turbulent behavior (Exhibit 12) which is favorable for both the gas and liquid side mass transfer. The sudden change of the bubbles path and shape cause even well mixing of gas in the bubbles in addition to more efficient mixing in the liquid phase. This can be also seen in photographs taken from the bubbles in Exhibit 12.

4.6 | The effect of temperature

The effect of temperature on absorption capacity is shown in Exhibit 13. The 3D surface is plotted for gas flow rate of 5 and pore size of 1.0 mm. It is clear that the temperature effect on absorption capacity at the tested range was not so significant.

The plot of absorption capacity versus pore sizes in Exhibit 13 on capacity at different pore sizes for gas flow rate of 6.0 L min⁻¹ and absorbent concentration of 20.0 vol%. In this case the temperature effect seems significant especially at bigger 1.5 mm pore size. The increase of temperature from 20.0 to 30.0°C at 1.5 mm pore size would increase the absorption capacity by 22.7%. The effect of temperature can be attributed to the higher mass transfer rate at higher temperatures.

The positive effect of temperature on the K_{Ga} is shown in Exhibit 14. It is well-known from mass transfer theories that the diffusivity of gas is in direct relation with temperature. The temperature therefore has positive effect at this range because of increased diffusivity of CO₂ in both gas phase and water liquid phase which was previously formulated by Versteeg et al. (1987). On the contrary, the exothermic nature of reaction pushes the reaction toward gaseous CO₂ or reactants side (Equations (19)–(22)). The enthalpy of CO₂ absorption in MEA solution was studied by Kim and Svendsen (2007) where for loading ranges of 0.1 to 1.0 mol CO₂/mol MEA at 40°C with 30 wt% MEA, 80 to 120 kJ mol⁻¹ absorbed CO₂ was reported. The regeneration of MEA solution is followed at high temperatures in a stripping process. Positive effect of temperature was also reported in (Maceiras et al., 2008) for similar ranges of temperature.

4.7 | Optimized process condition

The response surface methodology provides the opportunity of obtaining optimized condition based on the designed model (Aguirre-Fierro et al., 2020). These are (Exhibit 15) solutions at the range of defined variables including gas flow rate at 4.0–6.0 L min⁻¹, absorbent concentration at 10.0–30.0 vol%, diffuser pore size at 0.5–1.5 mm, and the temperature to be at the range of 20.0–30.0°C. The estimated maximized value for absorption capacity was also limited to the range of 27.0–120.0 g CO₂/kg MEA as was observed experimentally. The K_{Ga} was set to 3–13 range where maximum desirability could be achieved. The application of model for a range beyond the validity range of the

model may cause erroneous results. The results for optimization step is summarized in Exhibit 15. Three scenarios were applied including: (1) maximum absorption capacity, (2) maximum overall mass transfer coefficient, K_{GA} and (3) maximized absorption capacity and K_{GA} simultaneously. The obtained optimized values for first and second scenario do not match which is to say when the maximum capacity is the desired target the K_{GA} would fall down to 34.0 min^{-1} . From an application point of view, a process with highest absorption capacity and a short process time is desired. Therefore, third scenario for maximized both absorption capacity and K_{GA} was applied. Interestingly, the obtainable value for K_{GA} was high as 37.5 min^{-1} where an obtainable absorption capacity of $120.5 \text{ g CO}_2/\text{kg MEA}$ was predicted.

A gas flow rate of 5.9 L min^{-1} , MEA solution of 29.6 vol%, diffuser pore size of 0.5 mm and temperature of 20.6°C was the suggested optimized values. The obtained result was compared with other studies findings as given in Exhibit 16. To find a study with the same reactor type, geometry and operation range is almost impossible because the objectives in different studies are not the same. In general, our results is consistent with findings of Sheyda and Barati where a $0.63 \text{ kmol h}^{-1} \text{ m}^{-3} \text{ kPa}^{-1}$ was reported for mass transfer coefficient. A very high value of $4.98 \text{ kmol h}^{-1} \text{ m}^{-3} \text{ kPa}^{-1}$ as reported in (Rashidi et al., 2020) is not comparable with this studies result which may be related to the out of range answers of the optimization of the tuned model. Unfortunately, in RSM, many different scenarios are suggested mathematically as optimized result where many of them may not be obtainable practically. In this study, the solutions within the range of experiment variables were considered as possible practical solution.

5 | CONCLUSION

RSM is a powerful methodology for the study of carbon dioxide absorption in MEA solution. The factors must be adjusted so carefully to obtain the highest efficiencies. The results of the present study clearly showed that for a CO_2 absorption process where both absorption capacity and the rate of process is equally important, implementation of a RSM in an optimization study is inevitable. There could be interactions between the variables which could be distinguished in this approach. Very promising absorption capacity of $120.5 \text{ g CO}_2/\text{kg MEA}$ might be obtained at high mass transfer rates. A gas flow rate of 5.9 L min^{-1} , MEA solution of 29.6 vol%, diffuser pore size of 0.5 mm and temperature of 20.6°C was the suggested optimized values. Practically it is very important to have both absorption capacity and mass transfer rate high to reduce the final regeneration costs. This study shows that a two factor optimization with a robust RSM methodology is a successful approach for proposed application.

ACKNOWLEDGMENTS

This project was funded by Anadolu University under project no. 1706F386.

DATA AVAILABILITY STATEMENT

The data that support the findings of this study are openly available in manuscript.

ORCID

Ayşe Gul  <https://orcid.org/0000-0002-7924-8396>

REFERENCES

- Adeosun, A., Hadri, N. E., Goetheer, E., & Zahra, M. A., Absorption of CO_2 by Amine Blends Solution: An Experimental Evaluation. (2013).
- Aguirre-Fierro, A., Ruiz, H. A., Cerqueira, M. A., Ramos-González, R., Rodríguez-Jasso, R. M., Marques, S., & Lukasik, R. M. (2020). Sustainable approach of high-pressure agave bagasse pretreatment for ethanol production. *Renewable Energy*, 155, 1347–1354.
- Ali, B. S., & Aroua, M. (2004). Effect of piperazine on CO_2 loading in aqueous solutions of MDEA at low pressure. *International Journal of Thermophysics*, 25(6), 1863–1870.
- Aronu, U. E., Ghondal, S., Hessen, E. T., Haug-Warberg, T., Hartono, A., Hoff, K. A., & Svendsen, H. (2011). Equilibrium in the H_2O -MEA- CO_2 system: New data and modeling. in 1st Post Combustion Capture Conference, Abu Dhabi, Paper.
- Aronu, U. E., Gondal, S., Hessen, E. T., Haug-Warberg, T., Hartono, A., Hoff, K. A., & Svendsen, H. F. (2011). Solubility of CO_2 in 15, 30, 45 and 60 mass% MEA from 40 to 120°C and model representation using the extended UNIQUAC framework. *Chemical Engineering Science*, 66(24), 6393–6406.
- Aronu, U. E., Gondal, S., Hessen, E. T., Huah-Werberg, T., Hartono, A., Hoff, K. A., & Svendsen, H. F. (2011). Solubility of CO_2 in 15, 30, 45 and 60 mass% MEA from 40 to 120°C and model representation using the extended UNIQUAC framework. *Chemical Engineering Science*, 66(24), 6393–6406.
- Aroonwilas, A., & Veawab, A. (2004). Characterization and comparison of the CO_2 absorption performance into single and blended alkanolamines in a packed column. *Industrial & Engineering Chemistry Research*, 43(9), 2228–2237.
- Azari, A., Nabizadeh, R., Mahvi, A. H., & Nasseri, S. (2021). Magnetic multi-walled carbon nanotubes-loaded alginate for treatment of industrial dye manufacturing effluent: Adsorption modelling and process optimisation by central composite face-central design. *International Journal of Environmental Analytical Chemistry*, 1–21.
- Azari, A., Nabizadeh, R., Mahvi, A. H., & Nasseri, S. (2022). Integrated Fuzzy AHP-TOPSIS for selecting the best color removal process using carbon-based adsorbent materials: Multi-criteria decision making vs. systematic review approaches and modeling of textile wastewater treatment in real conditions. *International Journal of Environmental Analytical Chemistry*, 102(18), 7329–7344.
- Benson, S. M., & Orr, F. M. (2008). Carbon dioxide capture and storage. *MRS Bulletin*, 33(4), 303–305.
- Bernhardsen, I. M., & Knuutila, H. K. (2017). A review of potential amine solvents for CO_2 absorption process: Absorption capacity, cyclic capacity and pKa. *International Journal of Greenhouse Gas Control*, 61, 27–48.
- Chen, P. C., & Liao, C.-C. (2014). A study on CO_2 absorption in bubble column using DEEA/EEA mixed solvent. *International Journal of Engineering Practical Research*, 3(4), 78.
- Chen, C., Luo, Y. X., & Cai, W. (2015). CO_2 Capture Using Monoethanolamine in a Bubble-Column Scrubber. *Chemical Engineering & Technology*, 38(2), 274–282.
- Chen, P.-C., Shi, W., Du, R., & Chen, V. (2008). Scrubbing of CO_2 greenhouse gases, accompanied by precipitation in a continuous bubble-column scrubber. *Industrial & Engineering Chemistry Research*, 47(16), 6336–6343.

- Choi, W.-J., Seo, J.-B., Jang, S.-Y., Jung, J.-H., & Oh, K.-J. (2009). Removal characteristics of CO₂ using aqueous MEA/AMP solutions in the absorption and regeneration process. *Journal of Environmental Sciences*, 21(7), 907–913.
- D'Alessandro, D. M., Smit, B., & Long, J. R. (2010). Carbon dioxide capture: Prospects for new materials. *Angewandte Chemie International Edition*, 49(35), 6058–6082.
- Dashtian, K., Zare-Dorabei, R., Jafarinia, R., & Tehrani, M. S. (2017). Application of central composite design for optimization of preconcentration and determination of La (III) ion in water samples using the SBA-15-HESI and SBA-15-HESI-Fe3O4-NPs sorbents. *Journal of Environmental Chemical Engineering*, 5(5), 5233–5240.
- Dean, A., Voss, D., & Draguljić, D. (2017). *Response Surface Methodology, in Design and Analysis of Experiments*. (pp. 565–614): Springer International Publishing.
- Fadillah, G., & Saleh, T. A. (2022). Advances in mesoporous material for adsorption and photoconversion of CO₂ in environmental pollution: Clean environment and clean energy. *Sustainable Chemistry and Pharmacy*, 29, 100812.
- Hemmati, A., & Rashidi, H. (2019). Optimization of industrial intercooled post-combustion CO₂ absorber by applying rate- base model and response surface methodology (RSM). *Process Safety and Environmental Protection*, 121, 77–86.
- Jaaafari, J., Ghozikali, M. G., Azari, A., Delkhosh, M. B., Javid, A. B., Mohammadi, A. A., Agarwal, S., Gupta, V. K., Sillanpää, M., Tkachev, A. G., & Burakov, A. E. (2018). Adsorption of p-Cresol on Al2O3 coated multi-walled carbon nanotubes: Response surface methodology and isotherm study. *Journal of Industrial and Engineering Chemistry*, 57, 396–404.
- Kim, I., & Svendsen, H. F. (2007). Heat of absorption of carbon dioxide (CO₂) in monoethanolamine (MEA) and 2-(aminoethyl) ethanolamine (AEEA) solutions. *Industrial & engineering chemistry research*, 46(17), 5803–5809.
- La Rubia, M. D., García-Abuín, A., Gómez-Díaz, D., & Navaza, J. M. (2010). Interfacial area and mass transfer in carbon dioxide absorption in TEA aqueous solutions in a bubble column reactor. *Chemical Engineering and Processing: Process Intensification*, 49(8), 852–858.
- Lashof, D. A., & Ahuja, D. R. (1990). Relative contributions of greenhouse gas emissions to global warming. *Nature*, 344(6266), 529.
- Li, T., Keener, T. C., & Cheng, L. (2014). Carbon dioxide removal by using Mg (OH)₂ in a bubble column: Effects of various operating parameters. *International Journal of Greenhouse Gas Control*, 31, 67–76.
- Liu, Y., Zhang, L., & Watanasiri, S. (1999). Representing Vapor–Liquid Equilibrium for an Aqueous MEA–CO₂ System Using the Electrolyte Nonrandom-Two-Liquid Model. *Industrial & Engineering Chemistry Research*, 38(5), 2080–2090.
- Lv, B., Guo, B., Zhou, Z., & Jing, G. (2015). Mechanisms of CO₂ Capture into Monoethanolamine Solution with Different CO₂ Loading during the Absorption/Desorption Processes. *Environmental Science & Technology*, 49(17), 10728–10735.
- Maceiras, R., Alvarez, E., & Cancela, M. A. (2008). Effect of temperature on carbon dioxide absorption in monoethanolamine solutions. *Chemical Engineering Journal*, 138(1-3), 295–300.
- Manzolini, G., Fernandez, E. S., Rezvani, S., Macchi, E., Goetheer, E. L. V., & Vlugt, T. J. H. (2015). Economic assessment of novel amine based CO₂ capture technologies integrated in power plants based on European Benchmarking Task Force methodology. *Applied Energy*, 138, 546–558.
- Navaza, J. M., Gómez-Díaz, D., & La Rubia, M. D. (2009). Removal process of CO₂ using MDEA aqueous solutions in a bubble column reactor. *Chemical Engineering Journal*, 146(2), 184–188.
- Nazerdeyami, S., & Zare-Dorabei, R. (2019). Simultaneous adsorption of Hg²⁺, Cd²⁺ and Cu²⁺ ions from aqueous solution with mesoporous silica/DZ and conditions optimise with experimental design: Kinetic and isothermal studies. *Micro & Nano Letters*, 14(8), 823–827.
- Pashaei, H., Ghaemi, A., & Nasiri, M. (2017). Experimental investigation of CO₂ removal using Piperazine solution in a stirrer bubble column. *International Journal of Greenhouse Gas Control*, 63, 226–240.
- Pashaei, H., Ghaemi, A., Nasiri, M., & Karami, B. (2020). Experimental Modeling and Optimization of CO₂ Absorption into Piperazine Solutions Using RSM-CCD Methodology. *ACS Omega*, 5(15), 8432–8448.
- Peng, Y., Zhao, B., & Li, L. (2012). Advance in post-combustion CO₂ capture with alkaline solution: A brief review. *Energy Procedia*, 14, 1515–1522.
- Pszczółkowski, W., Pszczołkowska, A., Romanowska-Duda, Z., & Grzesik, M. (2015). Microalgae as efficient feedstock for biorefinery. *Acta Innovations*, 14, 17–25.
- Putta, K. R., Svendsen, H. F., & Knuutila, H. K. (2017). Kinetics of CO₂ absorption in to aqueous MEA solutions near equilibrium. *Energy Procedia*, 114, 1576–1583.
- Rahimi, M., Valeh-e-Sheyda, P., & Rashidi, H. (2017). Statistical optimization of curcumin nanosuspension through liquid anti-solvent precipitation (LASP) process in a microfluidic platform: Box-Behnken design approach. *Korean Journal of Chemical Engineering*, 34(11), 3017–3027.
- Rashidi, H., Valeh-e-Sheyda, P., & Sahraie, S. (2020). A multiobjective experimental based optimization to the CO₂ capture process using hybrid solvents of MEA-MeOH and MEA-water. *Energy*, 190, 116430.
- Roger, B. R. (1930). Process for separating acidic gases. Google Patents.
- Sada, E., Kumazawa, H., Lee, C., & Fujiwara, N. (1985). Gas-liquid mass transfer characteristics in a bubble column with suspended sparingly soluble fine particles. *Industrial & Engineering Chemistry Process Design and Development*, 24(2), 255–261.
- Sahraie, S., Rashidi, H., & Valeh-e-Sheyda, (2019). An optimization framework to investigate the CO₂ capture performance by MEA: Experimental and statistical studies using Box-Behnken design. *Process Safety and Environmental Protection*, 122, 161–168.
- Saleh, T. A. (2022a). Nanomaterials and hybrid nanocomposites for CO₂ capture and utilization: Environmental and energy sustainability. *RSC advances*, 12(37), 23869–23888.
- Saleh, T. A. (2022b). Organic-inorganic hybrid nanocomposites for the photoreduction of CO₂: Environment and energy technologies. *Bulletin of Materials Science*, 45(4), 222.
- Saleh, T. A., Rachman, I. B., & Ali, S. A. (2017). Tailoring hydrophobic branch in polyzwitterionic resin for simultaneous capturing of Hg (II) and methylene blue with response surface optimization. *Scientific Reports*, 7(1), 1–15.
- Sebeia, N., Jabli, M., Ghanmi, H., Ghith, A., & Saleh, T. A. (2019). Effective dyeing of cotton fibers using Cynomorium coccineum L. peel extracts: Study of the influential factors using surface response methodology. *Journal of Natural Fibers*, 21–23.
- Shuangchen, M., Gongda, C., Sijie, Z., Tingting, H., & Weijing, Y. (2016). Mass transfer of ammonia escape and CO₂ absorption in CO₂ capture using ammonia solution in bubbling reactor. *Applied energy*, 162, 354–362.
- Tippayawong, N., & Thanompangchart, (2010). Biogas quality upgrade by simultaneous removal of CO₂ and H₂S in a packed column reactor. *Energy*, 35(12), 4531–4535.
- Vaidya, D., & Kenig, E. Y. (2009). CO₂ capture by Novel Amine Blends. In (H. E. Alfadala, G. V. Rex Reklaitis, & M. M. El-Halwagi, Eds.), *Proceedings of the 1st Annual Gas Processing Symposium* (pp. 239–246). Elsevier: Amsterdam.
- Valeh-e-Sheyda, P., & Barati, J. (2021). Mass transfer performance of carbon dioxide absorption in a packed column using monoethanolamine-Glycerol as a hybrid solvent. *Process Safety and Environmental Protection*, 146, 54–68.
- Versteeg, G., Blauwhoff, P., & van Swaaij, W. M. (1987). The effect of diffusivity on gas-liquid mass transfer in stirred vessels. Experiments at atmospheric and elevated pressures. *Chemical Engineering Science*, 42(5), 1103–1119.

- Yeh, J. T., Pennline, H. W., & Resnik, K. (2001). Study of CO₂ absorption and desorption in a packed column. *Energy & Fuels*, 15(2), 274–278.
- Yuan, Y., & Rochelle, G. T. (2018). CO₂ absorption rate in semi-aqueous monoethanolamine. *Chemical Engineering Science*, 182, 56–66.

SUPPORTING INFORMATION

Additional supporting information can be found online in the Supporting Information section at the end of this article.

How to cite this article: Gul, A., Derakhshandeh, M., & Un, U. T. (2023). Optimization of carbon dioxide absorption in a continuous bubble column reactor using response surface methodology. *Environmental Quality Management*, 33(1), 79–93. <https://doi.org/10.1002/tqem.22020>